Comments on Inorganic Chemistry
Publication details, including instructions for authors and subscription information:
http://www.informaworld.com/smpp/title~content=t713455155

Development and Applications of an Extended-üuckel-Based Reactivity Index for Organometallic Complexes

Jacques Weber[a]; Dominique Stussi[a]; Peter Fluekiger[a]; Pierre-Yves Morgantini[a]; E. Peter Kündig[b]
[a] Department of Physical Chemistry, University of Geneva, Geneva 4, Switzerland [b] Department of Organic Chemistry, University of Geneva, Geneva 4, Switzerland

To cite this Article Weber, Jacques , Stussi, Dominique , Fluekiger, Peter , Morgantini, Pierre-Yves and Kündig, E. Peter(1992) 'Development and Applications of an Extended-üuckel-Based Reactivity Index for Organometallic Complexes', Comments on Inorganic Chemistry, 14: 1, 27 — 62
To link to this Article: DOI: 10.1080/02603599208048656
URL: http://dx.doi.org/10.1080/02603599208048656

Development and Applications of an Extended-Hückel-Based Reactivity Index for Organometallic Complexes

JACQUES WEBER, DOMINIQUE STUSSI,
PETER FLUEKIGER, PIERRE-YVES MORGANTINI
Department of Physical Chemistry,
University of Geneva,
30 quai Ernest-Ansermet,
1211 Geneva 4, Switzerland

E. PETER KÜNDIG
Department of Organic Chemistry,
University of Geneva,
30 quai Ernest-Ansermet,
1211 Geneva 4, Switzerland

Received April 21, 1992

A new formalism has been developed to evaluate from extended-Hückel wavefunctions the intermolecular interaction energy E_{int} between an organometallic substrate S and a model electrophile or nucleophile reactant R. Calculated as the sum of electrostatic, charge-transfer and exchange–repulsion components, E_{int} is used as a local reactivity index to interpret and predict the regio- and stereoselectivity of electrophilic and nucleophilic addition reactions to organometallics. The methodology developed incorporates molecular graphics as an important ingredient, as the reactivity index is represented using either: (i) a mapping onto the molecular surface by S by means of a color code or (ii) the generation of 3D isoenergy contour surfaces. This model is shown to be able to rationalize the activation of a benzene ring by complexation to the $Cr(CO)_3$ moiety and also to describe adequately the sequential addition of a carbanion nucleophile and of an electrophile to (η^6-benzene)tricarbonylchromium derivatives.

Comments Inorg. Chem.
1992, Vol. 14, No. 1, pp. 27–62
Reprints available directly from the publisher
Photocopying permitted by license only

Key Words: *organometallic reactivity, reaction potentials, molecular modeling, extended-Hückel theory, molecular graphics, semiempirical quantum chemistry*

1. INTRODUCTION

Computational chemistry has recently evolved from the stage of an esoteric tool employed by highly specialized scientists into a mature discipline with both its own research directions and important applications which are now well integrated within the daily activities of many chemists. Among these applications, molecular modeling and graphics are by no means the less useful ones as they allow, at different levels of sophistication, the study of molecular structure, function and interaction. In this context, molecular graphics (MG) techniques can be advantageously employed to build, represent and manipulate three-dimensional (3D) models of molecular structures and properties.[1-3] However, whereas such studies can be performed on a routine basis for organic compounds, the situation is somewhat different for transition metal complexes, such as organometallics, due to the considerable difficulties associated with a proper quantum chemical,[4] and empirical force field as well,[5] description of the main features of d-electron compounds. As an example, whereas the conformation of organic molecules comprising up to several hundred atoms can be built within a small amount of computer time using molecular mechanics models such as the popular MM2,[6] no such possibility exists yet for organometallics because of the difficulty of developing and generalizing an efficient force field to describe the various coordination modes and oxidation numbers of transition metals in such systems. We started some years ago a project aiming at the development of a molecular modeling system for organometallics.[7] Our purpose was to develop a computationally simple model so as to achieve rationalizations of the structure and properties of large systems within a reasonable amount of computer time. To this end, the model builder module is based on the modified extended-Hückel (EH) procedure proposed by Anderson and Hoffmann[8] and recently reformulated by Calzaferri *et al.*[9] We are in the phase of parametrizing this formalism for organometallic complexes and preliminary results obtained for metallocenes and carbonyl compounds

are promising. On the other hand, most of our methodological developments dealing with electronic structure and properties have been completed and integrated within the MOLCAD package developed by Brickmann.[10] They are also based on the EH method,[11] which is well known to lead to good qualitative, and in many cases semi-quantitative, results for transition metal complexes. In this paper, we would like to present and discuss the major aspects of these developments devoted to the calculation of a reactivity index for organometallics.

Indeed, in addition to the calculation of EH molecular orbitals (MOs), and their subsequent representation using 3D solid models, our molecular modeling system allows mainly the calculation of reaction potentials as intermolecular interaction energies E_{int} between an organometallic substrate and an incoming model reactant representative of an electrophile or of a nucleophile. Our purpose here is to have at hand a convenient reactivity index for organometallics, analogous to the popular molecular electrostatic potential (MEP)[12] which has met with considerable success in modeling organic reaction mechanisms[13] or in drug design applications.[14] The problem is that we have recently found[7] that the electrostatic component alone, i.e., the MEP itself, is not always sufficient for a proper description of reaction mechanisms involving the organometallic substrate S and an incoming reactant R with electrophilic or nucleophilic character. As such processes, which are basically due to the activation of organic ligands by coordination to transition metal atoms, represent an important class of reaction mechanisms in organometallic chemistry, we found it necessary to develop this new reactivity index by including the predominant components of E_{int} in addition to the electrostatic one.

As there is generally an important charge transfer (CT) between the d shell of the transition metal atom(s) of S and the orbitals of R, it is necessary to take into account the corresponding energy, which can be of the same order of magnitude as the electrostatic component. The CT mechanism is essentially due to orbital overlap and it has to be quantified using a MO model. As the frontier orbital theory could be misleading for the interpretation and prediction of organometallic reactivity because of the presence of several closely spaced energy levels in the region of both highest occupied MO (HOMO) and lowest unoccupied MO (LUMO),[15]

we turned to a procedure involving an EH calculation of the S-R supermolecule. In terms of computer time, this is the most demanding part of the calculations of E_{int}, as it has to be repeated for all the positions of R in the vicinity of S. Finally, whereas developments aiming at the calculation of the polarization component of E_{int} are still in progress, the last term which has been included in E_{int} is the exchange–repulsion energy. To this end, an empirical potential based on the Buckingham approximation has been used. Applied to a large number of nucleophilic and electrophilic addition or substitution reaction mechanisms in organometallic chemistry,[7,16–19] this model has been shown to be able to rationalize and generally predict the regioselectivity and energetics of such reactions. This indicates that additional energy components, such as polarization, would most probably not affect the qualitative trends of our results.

After a brief description of the theoretical model used, this Comment will concentrate on the rationalization of the mechanism of activation of arenes by a metal containing moiety such as $Cr(CO)_3$. Then the results of investigations of sequential additions of carbon nucleophiles and electrophiles to (η^6-benzene)tricarbonylchromium will be presented.

2. METHOD

In order to describe the reactive properties of substrate S in presence of reactant R, we use a local reactivity index made of the S-R intermolecular interaction energy, expressed as a sum of several components:

$$E_{int}(\mathbf{r}) = E_{es}(\mathbf{r}) + E_{ct}(\mathbf{r}) + E_{ex}(\mathbf{r}) \qquad (1)$$

where $\mathbf{r}$ specifies the position of the incoming reactant in the vicinity of the organometallic substrate, E_{es}, E_{ct} and E_{ex} being electrostatic, charge-transfer and exchange–repulsion energy components, respectively.

To keep the model computationally simple, we assume that selection of the most favorable region(s) of S to be attacked by R

occurs at rather large distances, well in advance of the transition state, so that geometrical distortions of S are negligible. This assumption is commonly made when modeling organic reactions using the MEP reactivity index.[13,14,20-23] In our case, i.e., for organometallic reaction mechanisms, we simply have to add a CT component to the MEP as the overlap integrals involving the d orbitals of metal atom(s) can be rather important at such distances and therefore lead to a non-negligible E_{ct} energy. This is especially true for electrophilic addition reactions, as exemplified by ferrocene where the MEP component alone predicts protonation on the ligand ring while introduction of E_{ct} changes completely the selectivity and, in agreement with experiment, favors the metal site.[7,24,25]

A convenient molecular graphics representation of the reactive properties of S is then provided by the construction and display of the molecular surface[26] of S color-coded according to E_{int} values, which leads to an immediate perception of the most favorable regions for S-R interaction.[27] However, this simple procedure may be inadequate to locate the global minimum of E_{int} among competing sites and, in many applications, it is useful to estimate the position of global (i.e., the most reactive site) and local minima as well of E_{int} in the whole molecular volume, without being restricted to the molecular surface. To this end, the molecule is immersed into a three-dimensional grid box and E_{int} is evaluated at each grid point. Then, isoenergy surfaces of E_{int} are displayed as 3D solid lobes representative of the spatial distributions of the sites of attack, in much the same was as suggested by Surcouf and Mornon for the construction of van der Waals signatures.[28]

It is important to choose a simple, though realistic, model for the reactant R, as the computer time required to evaluate E_{int} increases rapidly as a function of the complexity of R. In order to obtain E_{int} values that are dependent on the position of R only in the vicinity of S, and not on its orientation, two spherically symmetric model reactants have been selected: a proton with a virtual 1s orbital for the electrophile and an H^- hydride ion for the nucleophile. Let us turn now to the approximations we developed for the various components of E_{int}.

Electrostatic Component

In the case of electrophilic attack, E_{es} is equal to the MEP of substrate S[12]:

$$E_{es}(\mathbf{r}) = \sum_{A} Z_A/|\mathbf{r} - \mathbf{r}_A| - \sum_{\mu} \sum_{\nu} P_{\mu\nu} \langle \mu|1/r|\nu\rangle \qquad (2)$$

where the first term corresponds to the nuclear repulsion, the summation running over all atoms A of S, with nuclear charge Z_A located in $\mathbf{r}_A$. The second term originates from the electronic attraction, $P_{\mu\nu}$ being the first-order density matrix element corresponding to atomic orbitals (AOs) χ_μ and χ_ν, and $\langle \mu|1/r|\nu\rangle$ being defined as

$$\langle \mu|1/r|\nu\rangle = \int \chi_\mu(\mathbf{r}') \frac{1}{|\mathbf{r} - \mathbf{r}'|} \chi_\nu(\mathbf{r}')\, d\mathbf{r}'. \qquad (3)$$

In case of nucleophilic attack, we may reasonably assume that the electrostatic interaction between S and the H^- ion reduces to that between S and a negative point charge, which is obviously correct for rather large S-R distances where the so-called penetration integrals vanish. Several test calculations have shown this to be the case when R is at a distance larger than roughly 2.0 Å from any atom of S. For nucleophilic attack, the electrostatic component is, therefore, given by $-E_{es}$ (Eq. (2)).

As the calculation of $\langle \mu|1/r|\nu\rangle$ integrals using the EH basis of atomic orbitals is time-consuming because they are of Slater type, we approximate the MEP using the neglect of diatomic differential overlap (NDDO) scheme,[29] according to which the second right-hand term of Eq. (2) becomes

$$\sum_{\mu} \sum_{\nu} P_{\mu\nu}\langle \mu|1/r|\nu\rangle = \sum_{A} \sum_{\mu \in A} \sum_{\nu \in A} P_{\mu_A\nu_A}\langle \mu_A|1/r|\nu_A\rangle. \qquad (4)$$

The first summation is over all atoms A of S. However, this requires the evaluation of the reduced density-matrix using orthogonalized AOs.

At this point, it seems legitimate to ask two questions: (i) Does it make sense to use an EH electron density, obtained from MOs

calculated without consideration of electron repulsion effects, to evaluate a MEP? (ii) If the answer to this question is yes, how much does the NDDO approximation influence the EH MEPs? In order to bring a clear answer to these questions and thereby to test our model, a comparison is presented here of the MEP of water, a well-known test case, calculated at the ab initio SCF and EH levels using STO-3G and the corresponding Slater-type basis orbitals, respectively. In addition, we have developed a numerical procedure, based on the integration scheme proposed by Becke,[30] to calculate rigorously an EH MEP, which allows a comparison with the EH MEP obtained in the NDDO approximation (Eq. (4)). Again, water is the molecule chosen for this comparison.

Charge-Transfer Component

It is well known that organometallic substrates are often characterized by bands of closely spaced energy levels in both HOMO and LUMO regions.[15] This renders the use of frontier MOs only, in the evaluation of orbital or charge-transfer effects, as questionable. Instead, Brown *et al.* have suggested replacing the perturbation treatment by a complete EH calculation of the S-R supermolecule[15]; the so-called "orbital interaction energy" is obtained as the difference between the total energies of the supermolecule and those of the separate fragments. We have used the same approach in our model.

As EH total energies represent fairly comprehensively the sum of covalent energies within chemical bonds, the S-R charge-transfer energy may be approximated as

$$E_{ct}(\mathbf{r}) = E^{tot}(\text{S-R}, \mathbf{r}) - E^{tot}(\text{S}) - E^{tot}(\text{R}) \qquad (5)$$

where $E^{tot}(\text{X})$ represents the EH total energy of system X calculated as

$$E^{tot}(\text{X}) = \sum_i n_i \epsilon_i, \qquad (6)$$

n_i and ϵ_i being occupation number and energy, respectively, of the ith MO of X and $E^{tot}(\text{S-R}, \mathbf{r})$ being calculated for position $\mathbf{r}$ of

reactant R. It is to be noted that in the case of the H^- nucleophile reactant, $E_{ct}(\mathbf{r})$ may be positive or negative as well, as it results from the balance of: (i) attractive 2-electron interactions between the HOMO of R and the unoccupied MOs of S and (ii) repulsive 4-electron interactions between the HOMO of R and the occupied MOs of S.[31] The valence-state ionization energy (VSIE) H_{RR} of the 1s orbital of reactant H^- is therefore a critical parameter for the calculation of the charge-transfer component: moving H_{RR} downwards from a value close to the LUMO of S to more negative energies near the HOMO, i.e., transforming a soft nucleophile into a hard one, generally amounts to shifting E_{ct} from negative values to positive ones.

Exchange–Repulsion Component

In the case of electrophilic attack, there is no exchange–repulsion component in our model, as the reactant has no electrons. For nucleophilic attack, whereas in the case of color-coded molecular surfaces the reactivity index E_{int} usually comprises an exchange–repulsion component based on the hard-sphere approximation,[18] this procedure is no longer applicable to isoenergy surfaces as there is no molecular envelope to prevent the reactant from collapsing on the nuclei of S. A more elaborate short-range exchange–repulsion function is therefore needed and we use a parametrized potential of Buckingham type[32]:

$$E_{ex}(\mathbf{r}) = 828'000 \sum_{A \in S} k_{AH^-} \exp\left[-13.587 \frac{|\mathbf{r} - \mathbf{r}_A|}{R_A + R_{H^-}}\right] \quad (7)$$

where the summation runs over all atoms A of S, located in $\mathbf{r}_A$, k_{AH^-} being an energy parameter depending on atom A and H^- ion, R_A and R_{H^-} being the van der Waals radii of atom A and H^- ion, respectively.[33] In Eq. (7), E_{ex} is expressed in kcal/mol and the values of the parameters have been taken from Eliel *et al.*[34] for first- and second-row atoms. For chromium atom, the following values have been chosen: $k_{Cr\text{-}H^-} = 0.52$ kcal/mole, $R_{Cr} = 1.94$ Å.[35]

Computational Details

Except for the comparison between EH and ab initio MEPs, where exponents corresponding to STO-3G orbitals were employed, all the EH calculations were performed using the single-zeta Slater-type AOs of Clementi and Roetti.[36] However, the d shell of transition metal atoms was described by the double-zeta function of the same authors. For all hydrogen atoms and for the reactant, a 1s exponent of 1.0 has been used. In the evaluation of E_{es} (Eq. (2)), the self-consistent charge and configuration (SCCC) procedure was employed,[37] with a quadratic dependence of the VSIEs H_{ii} of all the atoms, for the calculation of the first-order density matrix P of substrate S. In the calculation of E_{ct} (Eq. (5)), the SCCC procedure was used in a first step to evaluate E^{tot}(S); then, in a second step, E_{ct} was computed at each point **r** by performing a non-SCCC calculation of E^{tot}(S-R, **r**) with the H_{ii} resulting from the previous step. In the calculation of E_{ct} for organometallics, the VSIE of the reactant H_{RR} was chosen at ϵ_{HOMO} + 0.2 eV and ϵ_{LUMO} − 0.5 eV for electrophilic and nucleophilic addition, respectively, in agreement with previous calculations.[7,16-19] Actually, these choices are arbitrary and, as in all semiempirical models, they have been dictated by the best agreement with experiment. In any case, HOMO–LUMO gaps are generally small for organometallics (1–2 eV) and in general the choice of H_{RR} has only a small influence on the results. The situation is different for organic compounds where large HOMO–LUMO gaps may be found. In this case, modifying the H_{RR} parameter from a value close to the LUMO to another one close to the HOMO may significantly change the E_{ct} component. The H_{RR} parameter should therefore be carefully calibrated in calculations of organic compounds.

In this work, the geometries of all the compounds investigated have been kept frozen at their experimental values. This means that our model does not account for the geometrical distortions occurring during formation of the transition states and possible intermediates. Actually, our purpose is not to calculate accurate reaction paths, but rather to predict on a semi-quantitative basis the regio- and possibly stereoselectivity of the reaction mechanisms investigated. To this end, a study of long- to medium-range intermolecular interactions between substrate and reactant, based on

the mechanisms governing molecular recognition extended to organometallics, should be a reasonable starting point. Our model is therefore intended to describe both van der Waals and the initial stage of covalent interactions using reaction potentials calculated for undistorted fragments. In its present stage of development, the model should be considered as a preliminary attempt to rapidly and efficiently rationalize organometallic reactivity using a simple and coherent semi-empirical approach.

3. TESTS OF THE MODEL

As it should be the case for every new methodological development, especially when based on a semiempirical procedure, our formalism has been previously tested for several case studies.[7,16,38,39] In particular, we have shown that EH and ab initio SCF MEPs indeed exhibit similar features for small molecules and zeolites as well, even though the aforementioned orthogonalization of the atomic basis set, due to the use of the NDDO approximation, induces some spurious changes in the first-order reduced density matrix by transferring artificially to the diagonal terms the overlap populations arising through non-diagonal contributions. This results in a slight overestimation of the one-center contributions to the MEP and, therefore, in slightly too negative MEP minima in regions close to atoms. This trend is generally reversed when using the Mulliken approximation[40,41] to evaluate the one-electron attraction integrals (Eq. (3)) of the EH formalism:

$$\langle\mu|1/r|\nu\rangle = 1/2S_{\mu\nu}[\langle\mu|1/r|\mu\rangle + \langle\nu|1/r|\nu\rangle]. \quad (8)$$

In this case indeed, the orthogonality of atomic orbitals with different l-values on the same center leads to the neglect of some negative $P_{\mu\nu}\langle\mu|1/r|\nu\rangle$ contributions and, therefore, to higher EH MEP minima as compared with ab initio SCF calculations. As we have recently developed the numerical procedure mentioned in Section 2 to calculate an EH MEP without any further approximation, we present in Fig. 1 the contour levels of the MEP of water calculated in the EH (numerical, NDDO and Mulliken) and ab initio SCF formalisms using the same one-electron basis set

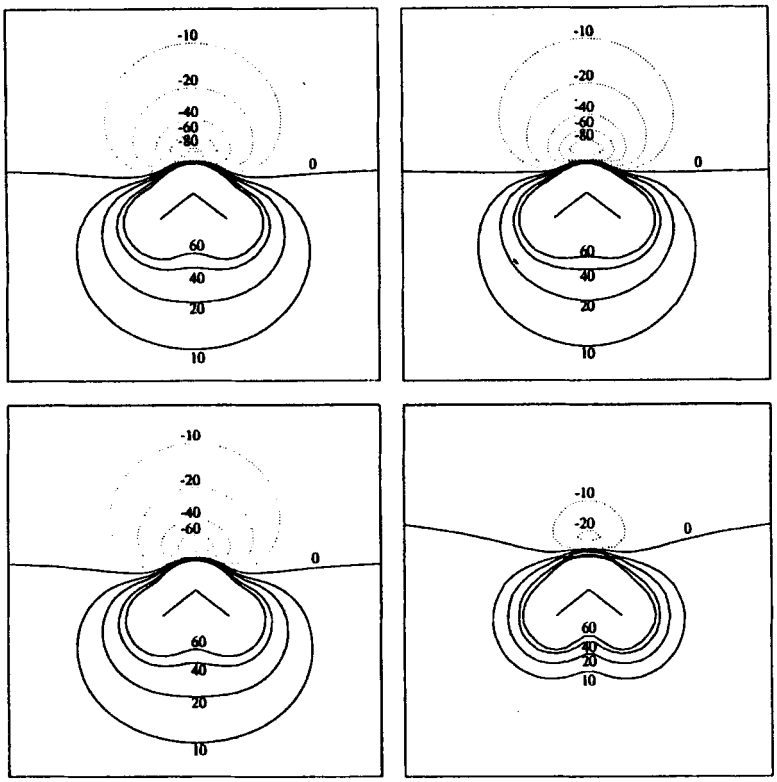

FIGURE 1 Contour maps of the MEPs calculated for water in the molecular plane. Positive (negative) contours are indicated by a solid (dotted) line; all values are in kcal/mol. Upper left: numerical EH (minimum −83 kcal/mol); upper right: NDDO EH (minimum −97 kcal/mol); lower left: ab initio SCF (STO-3G, minimum −70 kcal/mol), lower right: Mulliken EH (minimum −22 kcal/mol).

(STO-3G). It is immediately seen in Fig. 1 that both numerical and NDDO EH MEPs exhibit very similar features, the NDDO minimum lying as expected at a slightly lower energy than the numerical one. In addition, both of these MEPs are in good qualitative and quantitative agreement with the ab initio result which exhibits a minimum lying at a slightly higher energy. One may therefore conclude that, in spite of the SCCC procedure used in the present EH calculations, this model overestimates somewhat the polarity of the water molecule, but to an extent which is quite

comparable with the differences observed in MEP minima calculated at the ab initio SCF level using different basis sets.[42] However, it is seen in Fig. 1 that the EH MEP calculated using the Mulliken approximation underestimates significantly the absolute value of the minimum, i.e., it leads to a much too small attractive electrostatic interaction between water and the incoming proton. As the same effect has been previously noticed for other substrates,[16] this procedure should be disregarded for evaluating EH MEPs.

We are now in a position to answer the questions asked above concerning EH MEPs. Concerning the first one, these results show undoubtedly that an EH electron density can indeed be used to evaluate a MEP. Even though EH MOs have been obtained without consideration of electron repulsion effects, the electron density they lead to is close enough to that obtained using models taking this interaction into account to enable the calculation of very reasonable electrostatic potentials. Two reasons are probably at the origin of this behavior of EH solutions: (i) as stated by Ammeter *et al.*,[43] the construction of the EH secular determinant is such that "it leads in most cases to eigenvalues and eigenvectors that are qualitatively similar to those obtained from ab initio theories"; (ii) calculated as the sum of contributions arising from all the occupied valence orbitals, electron densities are probably less sensitive than other properties to the very details of the MOs themselves; in other words, there is certainly some compensation, or at least some averaging, of errors when calculating the electron density from EH MOs, and the corresponding MEPs do not reflect too sensibly the approximations inherent to the model. However, this statement does not equally apply to all semiempirical models, as previously reported by Culberson and Zerner[44] in support of the procedure they derived to calculate MEPs in the INDO approximation.

As to the second question of Section 2 regarding the influence of the NDDO approximation on EH EMPs, it is clearly seen in Fig. 1 that it is very small, leading mainly to a slightly more negative minimum when comparing with the "exact" numerical procedure. As in addition the use of this approximation leads to a considerable saving of computer time in the evolution of EH MEPs for large molecules such as organometallics, the NDDO scheme will be used throughout this Comment.

Further tests of the model can be carried out by examining the behavior of E_{int} itself and by comparing with S-R interaction energies calculated using the ab initio SCF method in the supermolecule approximation:

$$E_{int}(\text{S-R}) = E_{tot}(\text{S-R}) - E_{tot}(\text{S}) - E_{tot}(\text{R}). \qquad (9)$$

For the latter calculations, it is preferable to use large basis sets in order to reduce the well-known basis set superposition error.[45] It is true that this error could also affect our EH results, but only through the E_{ct} component which is obtained by subtracting the total energies of fragments from that of the supermolecule. However, correcting for these errors in the EH formalism would be nonsense in view of the large approximations inherent in this semiempirical model!

Water is known to protonate on the oxygen atom so as to form the pyramidal OH_3^+ oxonium ion. Although protonation occurs out of the molecular plane, in a direction corresponding roughly to the pπ lone pair,[46] we have chosen to calculate the E_{int} energy along the C_2 axis of the molecule because this direction lies in the plane of the molecule and the results may be directly compared with Fig. 1. In addition, this direction also reflects a strongly bonding interaction between the incoming proton and the pσ lone pair. The results displayed in Fig. 2 indicate that there is a very good agreement between interaction energies calculated at EH (using either the numerical or NDDO MEP) and ab initio SCF levels. Both the optimized position of proton and the minimum value of E_{int} compare fairly well in the two models, especially when using the numerical EH MEP, which gives further confidence in the approximate model. However, as could be expected from examination of Fig. 1, the minimum of E_{int} calculated using the Mulliken-approximated EH MEP is too shallow as compared with the ab initio result, which justifies our strategy to use NDDO EH MEPs.

As a test case for nucleophilic substitution, we have chosen the S_N2 reaction $H^- + CH_3F \rightarrow CH_4 + F^-$ which has been the subject of numerous theoretical studies.[47] It is now generally accepted that the backside attack, i.e., along the C_3 axis of CH_3F towards the face containing three hydrogen atoms (Fig. 3) is the most favorable

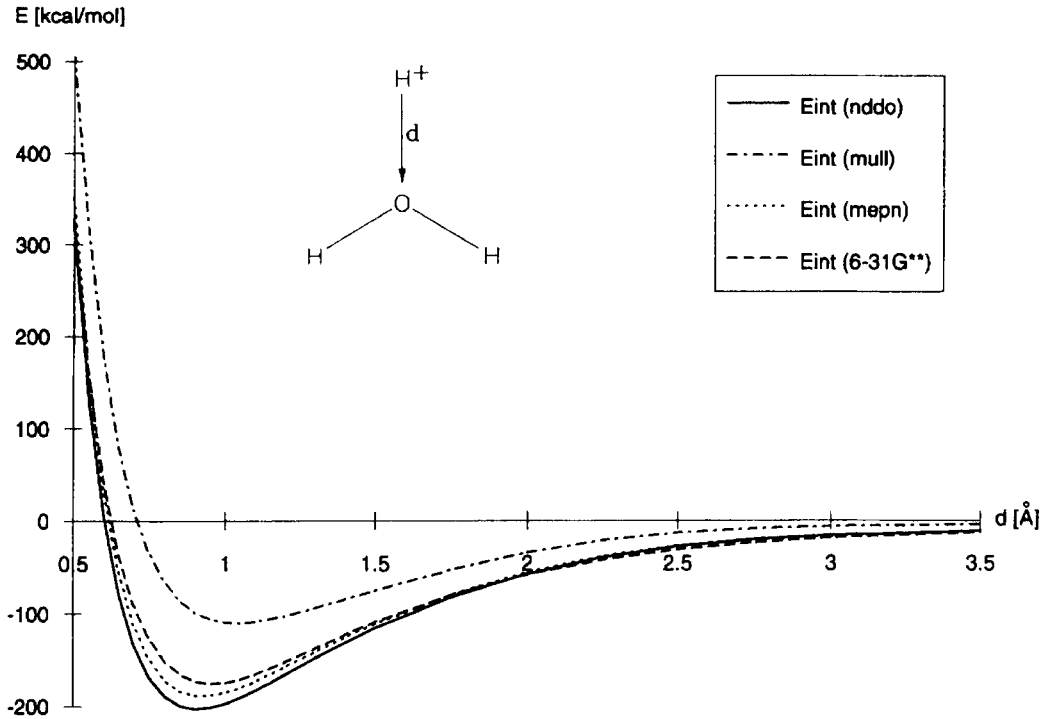

FIGURE 2 Interaction energies calculated for the $OH_2 + H^+ \rightarrow OH_3^+$ reaction as a function of distance between oxygen and the incoming proton in the molecular plane. Nddo, mull and mepn stand for EH interaction energies calculated using the NDDO, Mulliken and numerical electrostatic (MEP) components, respectively. 6-31G** stands for the ab initio SCF interaction energy calculated using the supermolecule approach and the 6-31G** basis set.

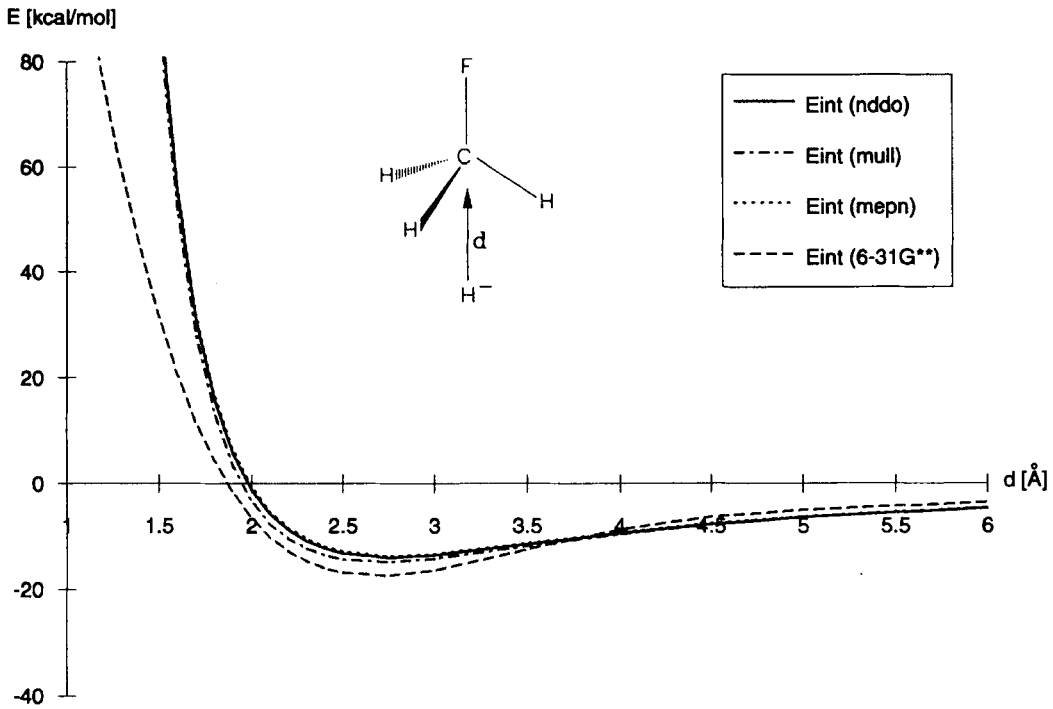

FIGURE 3 Interaction energies calculated for the $H^- + CH_3F \rightarrow CH_4 + F^-$ S_N2 reaction, in the backside case, as a function of distance between carbon and the incoming proton along the C_3 axis. For an explanation of the codes of the various curves, see Fig. 2.

one, the reaction path predicted by Dedieu and Veillard concluding to an energy barrier of 4 kcal/mol.[48] In our test calculations of this mechanism, we have evaluated both EH and ab initio SCF E_{int} energies as a function of distance d between H^- and the carbon center for the backside approach. As we are interested in the initial step of the mechanism only, we intentionally do not optimize the geometry of CH_3F for the different positions of the incoming nucleophile, which automatically leads to highly repulsive interaction energies when d is less than 2.0 Å. Again, it is seen in Fig. 3 that in these conditions both EH and ab initio curves are in very good agreement, especially as far as the bonding region of the curves are concerned. The repulsive parts of the profiles calculated using these two models, however, display some disagreement as the EH curves exhibit a much faster increase of E_{int} when d decreases. This has undoubtedly to be ascribed to the crude empirical potential we use for E_{ex}, but, as the long-range minima we are interested in are very similar in both EH and ab initio models, it is not necessary to refine our E_{ex} potential any further. These results therefore suggest that, for both electrophilic and nucleophilic addition reactions, the present model compares favorably with ab initio SCF results obtained using large polarized basis sets and we can now turn to applications devoted to organometallics.

4. ACTIVATION OF ARENES BY THE $Cr(CO)_3$ MOIETY

It is well known in organometallic chemistry that the electrophilic reactivity of arenes is remarkably increased by coordination to the $Cr(CO)_3$ moiety.[49-52] This observation is generally rationalized by inferring that metal–arene bonding leads to a net intramolecular charge transfer from the ring to the carbonyls, with the result that this compound is easily attacked by a nucleophile on the exo-face of the ring. For unsubstituted arenes such as benzene, which behave mostly as poor electrophiles, π-coordination to the metal system has been shown to have an effect similar to that of a nitro substituent in the σ-bond framework.[49,52] This allows us to understand why (η^6-benzene)tricarbonylchromium, **1** (Scheme 1), and related species have important synthetic applications in aromatic

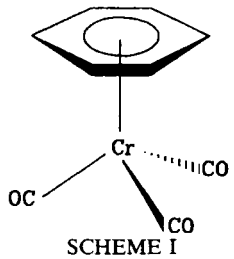

SCHEME I

chemistry, particularly in view of the preparation of regioselectively functionalized aromatics under mild conditions.[53,54]

In this Section, we would like to use our model in order to rationalize the basic mechanism of the enhanced electrophilic activity of benzene when coordinated to $Cr(CO)_3$. Our theoretical approach should indeed be able to provide a realistic description of this mechanism of activation using a combination of simple physical concepts and illuminating graphics. We have therefore calculated the interaction energy between substrate **1** and nucleophilic H^- reactant as a function of the position of the latter species on the molecular surface of **1** and Fig. 4 indeed shows that the most reactive site of **1** is located on the exo-face of the ligand ring, though the region with negative E_{int} values extends largely over the upper part of the surface towards the metal atom. The central and lower portions of the surface, however, are mostly unreactive, which indicates that nucleophilic addition is unlikely to take place on the metal or on the carbon atoms of CO groups, which parallels the experimental evidence.

For organometallic reaction mechanisms such as the one investigated here, some other local reactivity indices, generally cruder than the E_{int} property, may be used, namely gross atomic charges or frontier orbital (i.e., the LUMO in the case of a nucleophilic attack) charge density. Obviously, the first one applies to charge controlled mechanisms whereas the second one is a better descriptor of orbital controlled reactions and it has been suggested, on the basis of several pioneering test case studies,[55-57] that nucleophilic additions to organometallic species of $(polyene)_nM(L)_m$ type belong generally to the second group. Indeed, the metal atom in such complexes bears invariably the highest positive charge and, as it is not the most reactive site towards nucleophilic attack, a charge controlled mechanism must be ruled out.[57] This is con-

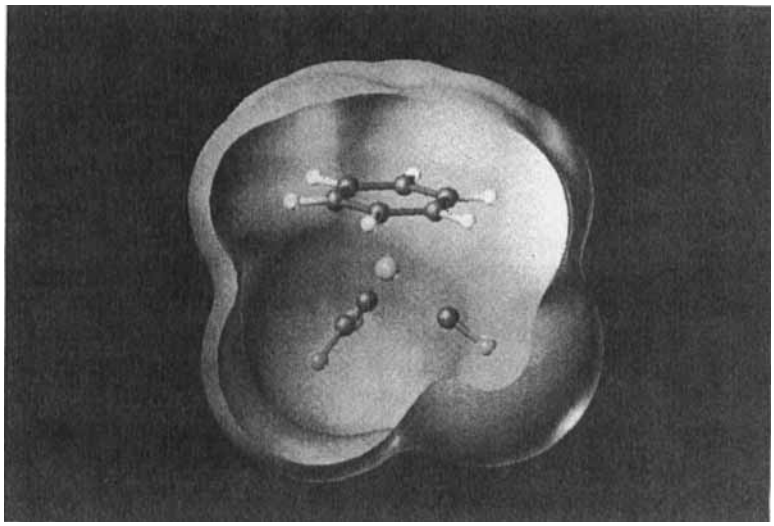

FIGURE 4 Solid model of the molecular surface of complex **1** colored according to the E_{int} reactivity index calculated for nucleophilic attack. (See Color Plate I at back of issue.)

firmed by Table I which displays the gross atomic charges of **1**. However, an orbitally controlled mechanism based on the localization of the LUMO alone does not apply either, as revealed by Fig. 5 which displays a solid model of one component of the degenerate LUMO of **1**. It is seen indeed that this orbital is mostly localized on metal and carbonyl ligands and the magnitude of its AO coefficients therefore does not correlate with the chemoselective attack on the ligand ring. This apparent failure of the frontier orbital model is due to the presence of low-lying unoccupied MOs located close to the LUMO and which should be taken into account in the orbital interaction procedure. As in our approach all the MOs of **1** may interact with the incoming nucleophile through the E_{ct} component, it is not surprising that the E_{int} index does correctly describe the selectivity of the reaction. In addition, our model equally applies to charge and orbitally controlled reactions as it rests on the simultaneous evaluation of both electrostatic and charge transfer interaction energies between the reactants.

Having thus verified that our model predicts adequately the

TABLE I

Comparison of EH results obtained for various metal-cycle distances ($d_{Cr\text{-}cycle}$) of Cr(benzene)$(CO)_3$.

$d_{Cr\text{-}cycle}$ (Å)		1.726 (equilibrium)	2.226	2.726	3.226	∞
Gross charge on						
Cr		0.621	0.487	0.431	0.417	0.414
C (carbonyle)		0.030	0.033	0.041	0.045	0.048
O		−0.208	−0.201	−0.193	−0.189	−0.186
C (benzene)		−0.013	−0.003	−0.004	−0.006	−0.008
H		−0.002	0.006	0.008	0.009	0.008
E_{int} minima (kcal/mol)						
On Cr	E_{es}	–[a]	–[a]	4.2	4.1	−23.5[b]
	E_{ct}	–	–	−11.5	−21.4	−42.3
	E_{ex}	–	–	4.4	6.5	10.2
	E_{int}	–	–	−2.9	−10.8	−55.6
On cycle	E_{es}	−23.3	−16.5	−8.8	−4.3	−0.3
	E_{ct}	4.0	1.7	0.8	0.4	0.1
	E_{ex}	0.4	0.1	0.0	0.0	0.0
	E_{int}	−18.9	−14.7	−8.0	−3.9	−0.2

[a]No minimum on Cr for this distance.
[b]Minimum located in anti position with respect to CO groups.

stereo- and chemoselectivity of the nucleophilic attack to **1**, let us turn now to the mechanism of activation of benzene when coordinating to the $Cr(CO)_3$ fragment. Figure 6 presents isoenergy surfaces of E_{int} calculated for both an isolated benzene ring and compound **1**. It is immediately seen that, as expected, an important change in reactivity accompanies benzene complexation: whereas for the isolated aromatic ring one observes slightly negative isoenergy envelopes centered on the C_6 axis on both sides of the molecular plane and representative of a weak van der Waals interaction, the situation changes dramatically for the coordinated ring. In the latter case, several imbricated surfaces are found at much lower energies, on the exo-face of the ring only, revealing a much stronger interaction with the incoming nucleophile. Actually, the colored isoenergy surfaces displayed in Fig. 6 do not require too many comments, as they reveal immediately, even to a non-specialized reader, that coordination confers important reactive properties to the exo-face of the ring. In our opinion, Fig.

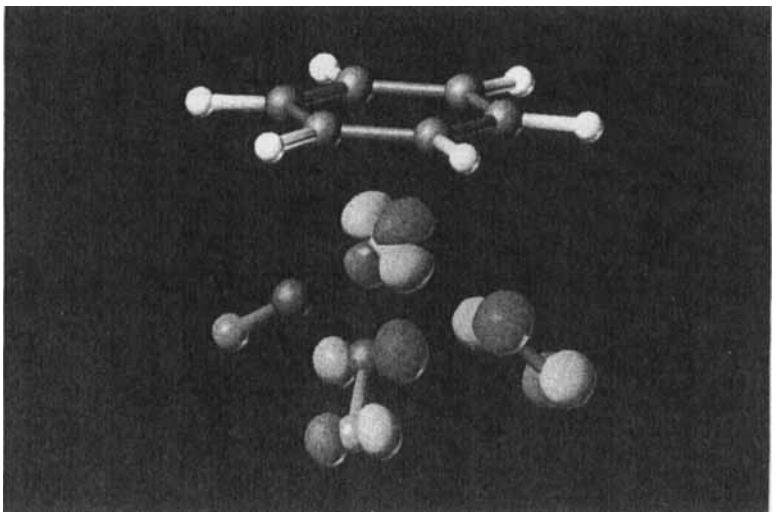

FIGURE 5 Solid model of the LUMO of complex **1**. Blue and yellow surfaces correspond to isovalues (±0.1 atomic units) of opposite signs. (See Color Plate II at back of issue.)

6 illustrates eloquently the advantages of using graphics rather than long listings of numbers!

We may open here a parenthesis to discuss briefly the influence of the calculation parameters on the results. Experience with the model has shown that the most critical parameters are the VSIE of reactant R, H_{RR}, and the van der Waals radius of nucleophile, R_{H^-}. Indeed, we have recently shown in the case of the (η^4-butadiene)$Fe(CO)_3$ complex that modifying H_{RR} by less than 0.5 eV so as to increase the hard character of nucleophile leads to displacing the regioselectivity from the terminal to the internal carbon of butadiene.[19] In the present case, no such effect has been observed and the isoenergy surfaces of E_{int} display only minor changes when lowering H_{RR} by as much as 1.8 eV within the 2.1 eV HOMO–LUMO gap of this compound. As to the effect of R_{H^-}, Fig. 7 shows that when reducing its value from 1.55 Å, the standard choice in our calculations,[58] to 1.20 Å, i.e., when shifting the exchange–repulsion positive energy component of E_{int} closer to the atoms of the substrate, additional minima appear on the exo-

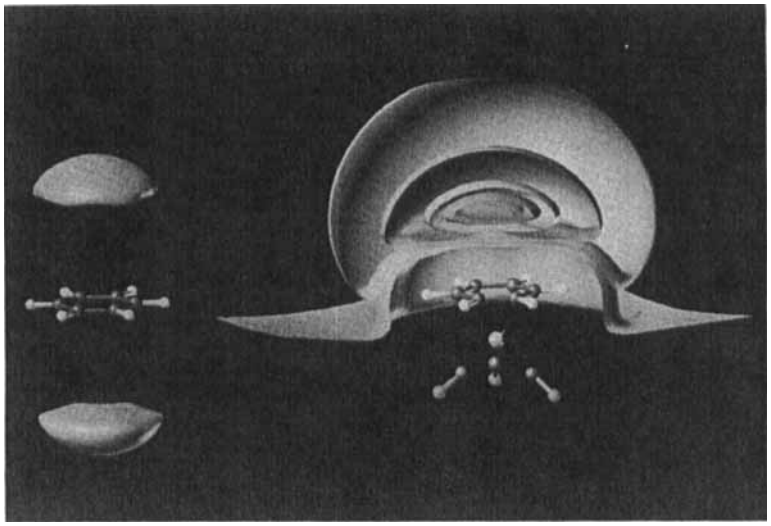

FIGURE 6 Structural models of benzene (left) and (η^6-benzene)$Cr(CO)_3$ (right) represented together with solid models of E_{int} isovalue surfaces calculated for nucleophilic attack (van der Waals radius of nucleophile: 1.55 Å). Color-coding of the surfaces: blue: −0.2, purple: −5.0, green: −10.0, yellow: −15.0, brown: −17.0 and red: −18.0 kcal/mol. (See Color Plate III at back of issue.)

face of the ligand ring. Located above the carbon atoms and closer to the ring, they can be interpreted as the initial stage of covalent minima corresponding to the formation of a cyclohexadienyl unit through the nucleophilic addition reaction. Clearly, an accurate description of these covalent minima would require us to allow for substrate distortion and also to improve the description of S-R interaction energy by developing a quantitatively accurate model, and this is undoubtedly out of the scope of the present investigation. However, it is interesting to see that this simple approach of reactivity is in principle able to lead to a qualitatively correct description of both long-range and the initial stage of short-range most favorable attractive interactions between substrate and reactant. This suggests that, for kinetically controlled mechanisms, i.e., in cases where the undistorted fragment approximation is not too crude, regioselectivity is mostly dictated by initial product selection occurring well in advance of the transition state[23] and mainly due to long-range favorable interactions. In other words, for this type

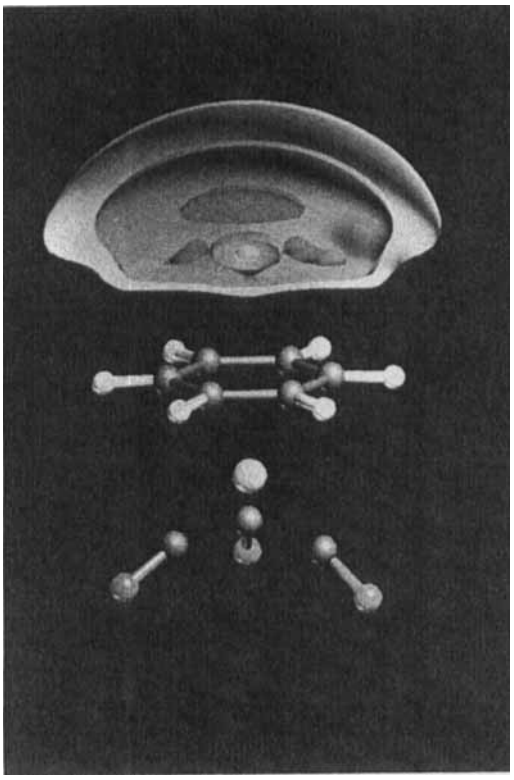

FIGURE 7 Structural model of (η^6-benzene)$Cr(CO)_3$ represented together with solid models of E_{int} isovalue surfaces calculated for nucleophilic attack (van der Waals radius of nucleophile: 1.20 Å). Color-coding of the surfaces: blue: −12.0, yellow: −15.0 and red: −18.5 kcal/mol. (See Color Plate IV at back of issue.)

of reaction, it is unlikely that long-range and short-range minima of a local reactivity index such as E_{int} would provide different descriptions of the regioselectivity of the mechanisms.

Following this digression on the influence of calculation parameters on the E_{int} minima, we now return to the activation of ligand ring in **1**. Possible approaches to rationalize the main features of Fig. 6 consist in (i) comparing the atomic charges of benzene and complex **1** and (ii) examining the various components of E_{int} calculated at the minima of the reactivity index. Table I presents these results, together with the same information obtained for

three vertical metal-to-ring distances intermediate between that of equilibrium in **1** (1.726 Å) and a large value corresponding to uncomplexed benzene and the $Cr(CO)_3$ fragment. These distances have been chosen as 2.226, 2.726 and 3.226 Å, respectively, and they are representative of situations of intermediate chemical bond formation between benzene and $Cr(CO)_3$. In addition, in order to enable the reader to rapidly localize the corresponding E_{int} minima for these intermediate distances, Fig. 8 displays the low-lying iso-energy lobes obtained in these three cases. Finally, Fig. 9 shows the similar result calculated for the $Cr(CO)_3$ fragment, which should enable us to simply and fully apprehend the origin of the enhanced electrophilic reactivity of benzene brought about by coordination.

Several quantum chemical studies of complex **1** have been previously reported[59–65]; they have been performed using various methods ranging from SCCC-EH[59–62] to CNDO/2[63,64] and ab initio

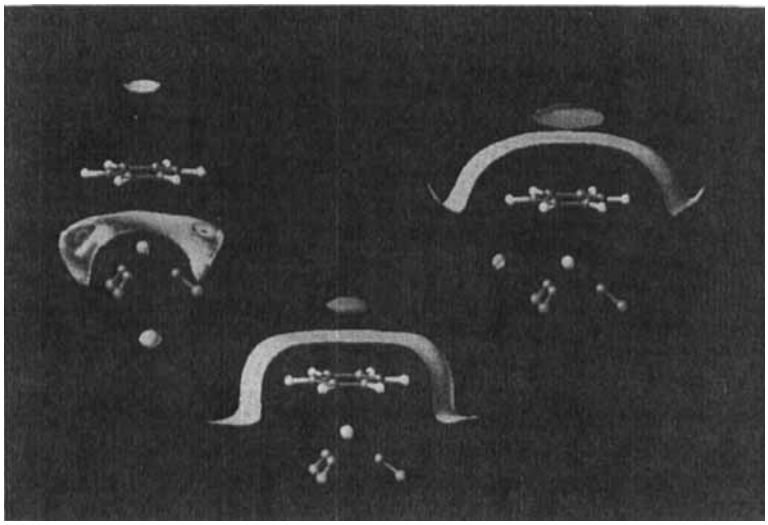

FIGURE 8 Structural models of (η^6-benzene)$Cr(CO)_3$ represented together with solid models of E_{int} isovalue surfaces calculated for nucleophilic attack (van der Waals radius of nucleophile: 1.55 Å) for three different metal-to-ring distances: 3.226 Å (upper left), 2.726 Å (upper right), 2.226 Å (lower part). Color-coding of the surfaces: blue −3.0 kcal/mol (in all cases), red: −9.0 kcal/mol (upper left), −7.0 kcal/mol (upper right), −13.0 kcal/mol (lower part). (See Color Plate V at back of issue.)

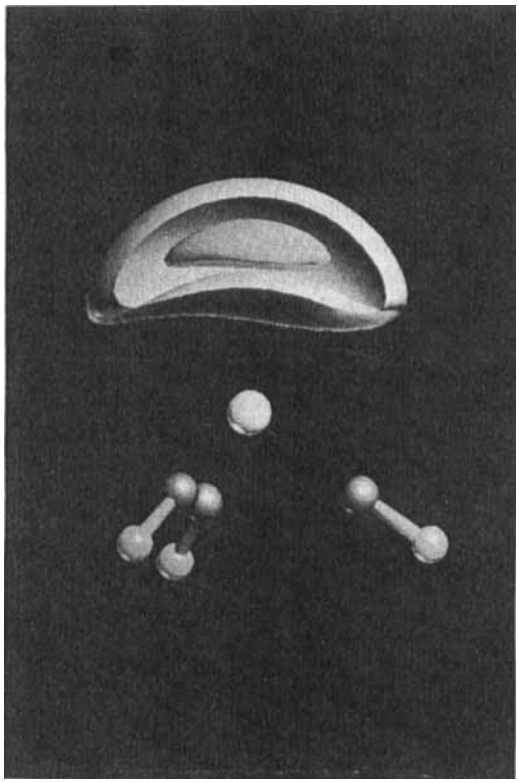

FIGURE 9 Structural model of the $Cr(CO)_3$ fragment represented together with solid models of E_{int} isovalue surfaces calculated for nucleophilic attack. Color-coding of the surfaces: yellow: −30 kcal/mol, red: −50 kcal/mol. (See Color Plate VI at back of issue.)

SCF.[65] In general, they lead to a coherent description of the characteristics of chemical bonding in the complex, though the gross charges calculated on the various atoms may differ significantly from one model to the other. As far as our results are concerned, it is seen in Table I that they lead to a positive charge on metal atom (+0.621) and to negative benzene (−0.090) and carbonyl (−0.178 each) ligands. Whereas these values are, as expected, in good agreement with those obtained by Brown *et al.*[60] in their SCCC-EH calculations performed with different parameters than the present ones, they are somewhat at variance with the ab initio

SCF results of Guest *et al.*[65] predicting much higher charges on metal (+2.08) and on carbonyl (−0.41 each). It is well known that, in any quantum chemical model, the derivation of atomic charges is somewhat arbitrary and, therefore, their values should be taken with caution. However, since the oxidation number of chromium in complex **1** is formally zero, the ab initio result of a +2.08 charge on this atom is questionable, as it seems that the one-electron basis set used in this model strongly overestimates the metal to ligand π back-donation. Similarly, the negative charge on chromium (−0.059) reported by Saillard *et al.*[63] from their CNDO/2 calculation might be due to a calculation artifact and results concluding to a small positive charge of the order of +0.5 on this atom, such as the present ones, are probably more realistic.

To address the question of benzene activation in **1**, it is necessary to briefly discuss the mechanism of chemical bonding in this complex. Without entering into too many details, our EH results together with the charges reported in Table I reveal moderate amounts of CO to Cr and benzene to Cr charge donations, essentially of σ and π nature, respectively, which are overcompensated by π Cr to CO and both σ and π Cr to benzene back-donations. This allows us to understand the negative charges borne by both types of ligands. However, the negative charge on CO in **1** is larger by 0.04, in absolute value, than that in $Cr(CO)_3$, which indicates that indeed Cr to CO π back-donation is enhanced by benzene coordination. Table I thus provides the numerical justification of the "net intramolecular charge transfer from the ring to the carbonyls" induced by the reaction:

$$C_6H_6 + Cr(CO)_3 \rightarrow (C_6H_6)Cr(CO)_3.$$

In addition, a detailed examination of the orbital populations of the C atoms of benzene before and after coordination to $Cr(CO)_3$ shows an increase of 2s population (+0.068) and simultaneously a decrease of 2pπ (−0.078), whereas the corresponding figures for 2pσ exhibit practically no change. This allows us to rationalize as follows the mechanism of benzene activation: coordination to $Cr(CO)_3$ induces a net π ligand to metal charge donation, leading to a corresponding increase of electrophilic reactivity in the exo (π) region of the ring (Fig. 3), and simultaneously a σ and π metal to ligand back-donation giving rise finally to a slightly negative

coordinated benzene. As expected, Table I shows that the mechanism takes place progressively along the $d_{Cr\text{-}cycle}$ reaction coordinate: moving the benzene moiety from an isolated species to a ligand at its equilibrium position in **1** results in smooth charge modifications from their initial to their final atomic values. Interestingly, examination of experimental electron deformation density maps reported for **1** shows that negative contours appear on the exo-face of benzene, which confirms that coordination leads to a net loss of electron density in this region.[66,67]

It may be useful to look at the evolution of the minima of E_{int} when going from isolated benzene (Fig. 6) and $Cr(CO)_3$ (Fig. 9) fragments to complex **1** through intermediate steps of complexation (Fig. 8). It is seen in Fig. 8 that the $Cr(CO)_3$ moiety exhibits a marked regioselectivity for nucleophiles along a direction coinciding with the C_3 axis of the molecule, in anti position with respect to CO groups. This explains the mode of coordination of benzene, which behaves indeed as a nucleophile (and not as an electrophile!) approaching $Cr(CO)_3$ with its molecular plane perpendicular to this C_3 axis. Examination of Table I shows that the E_{int} minimum on $Cr(CO)_3$ originates mainly from charge transfer ($E_{ct} = -42.3$ kcal/mol), the electrostatic contribution being roughly half of that. This is consistent with the soft electrophilic character of $Cr(CO)_3$, which is more likely to interact with incoming nucleophiles through an orbitally controlled mechanism. On the other hand, as mentioned above, free benzene is a poor electrophile with a very shallow E_{int} minimum lying at -0.2 kcal/mol. For the intermediate $d_{Cr\text{-}cycle}$ distances 3.226, 2.726 and 2.226 Å, the minimum on chromium is displaced from the C_3 axis to the equatorial plane (i.e., a horizontal plane containing the Cr atom) and simultaneously its energy raises significantly, with the result that this minimum is no longer found at 2.226 Å and below. However, in spite of its different location for these intermediate metal-cycle distances, the minimum on chromium still originates mainly from charge transfer interactions. Simultaneously, when gradually complexing benzene to $Cr(CO)_3$, it is seen in Fig. 8 and Table I that the minimum on the exo-face of the ring deepens considerably, with the result that it becomes the global minimum from 2.726 Å onwards. It is remarkable that this minimum has a purely electrostatic character, the E_{ct} component being repulsive at all distances. This is con-

firmed by Fig. 10, which displays the contour levels of $E_{es} + E_{rep}$ in a vertical plane for both an isolated benzene and complex **1**. The important depletion of electron density on the exo-face of benzene occurring through complexation, and reflected by the de-

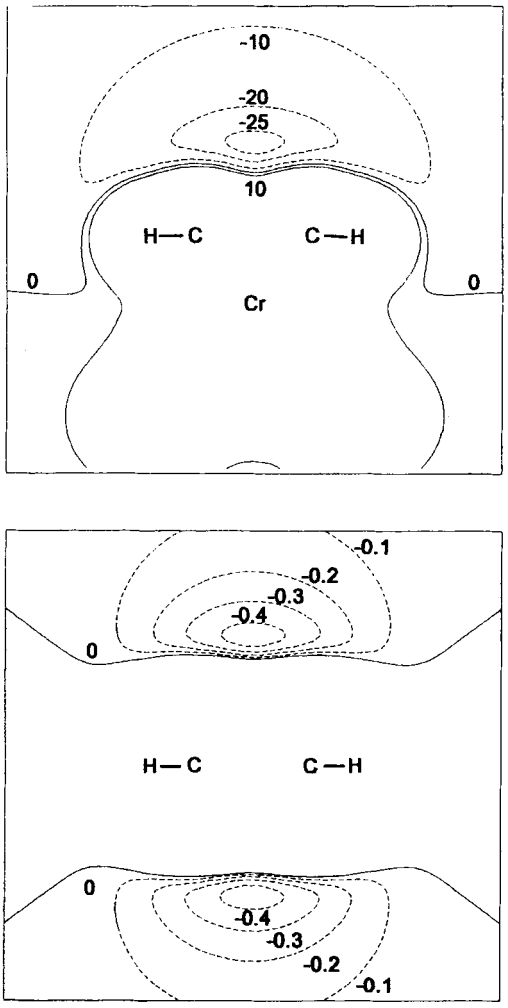

FIGURE 10 Contour maps of the $E_{es} + E_{ex}$ property calculated for nucleophilic attack of benzene (lower part) and (η^6-benzene)$Cr(CO)_3$ (upper part) in a vertical plane containing two CH groups of benzene; all values are in kcal/mol.

crease of carbon $2p\pi$ orbital population discussed above, is easily visualized as it results in much stronger attractive electrostatic interactions with the incoming hydride anion.

To summarize, the $Cr(CO)_3$ moiety activates the benzene ligand towards nucleophiles by gradually conferring to it most of its electrophilic character through complexation, mainly because of the net charge transfer arising from the ring to the metal and further to the carbonyls. However, in view of the very different nature of the complexing entities, the orbitally controlled reactivity of $Cr(CO)_3$ is modified in compound **1** into a charge controlled reactivity of the ring towards nucleophiles. It is therefore important to have at hand a model taking account of both processes to discuss the regioselectivity of such mechanisms in organometallic chemistry.

5. INVESTIGATIONS OF SEQUENTIAL ADDITIONS OF NUCLEOPHILES AND ELECTROPHILES TO (η^6-BENZENE)TRICARBONYLCHROMIUM

One of us has recently shown that trans-5,6-disubstituted cyclohexadienes **4** and **5** (Scheme 2) can be obtained via a one-pot reaction sequence involving the sequential addition of a nucleophile and an electrophile to (η^6-benzene)tricarbonylchromium derivatives **1a**–**1f**.[68–70] As seen in the previous section, our results predict that addition of a nucleophile such as the 2-methyl-1,3-dithiane anion to **1** takes place with a high stereoselectivity to the exo-face of the ligand ring, which is in total agreement with the X-ray crystallographic study of **2** (L = CO) (Scheme 2).[53] The conclusion remains valid when **1** is modified by substitution of a CO ligand by a phosphorous ligand,[70] even though this replacement could in principle drastically alter the reactivity of the complex.[71,72] Our objective here is to concentrate on the second part of the reaction sequence, namely the electrophilic addition to the anionic cyclohexadienyl complex **2**.

Experimentally, complexes **1a**, **1b** and **1c** were subjected to the "double addition" reaction of Scheme 2 where the electrophile used for the second addition was methyl- or ethyl-iodide, or, for the isolation of intermediate **3**, $ClSnPh_3$.[68,70] Then, X-ray analyses of the resulting complexes **3a** and **3c** have been performed in order

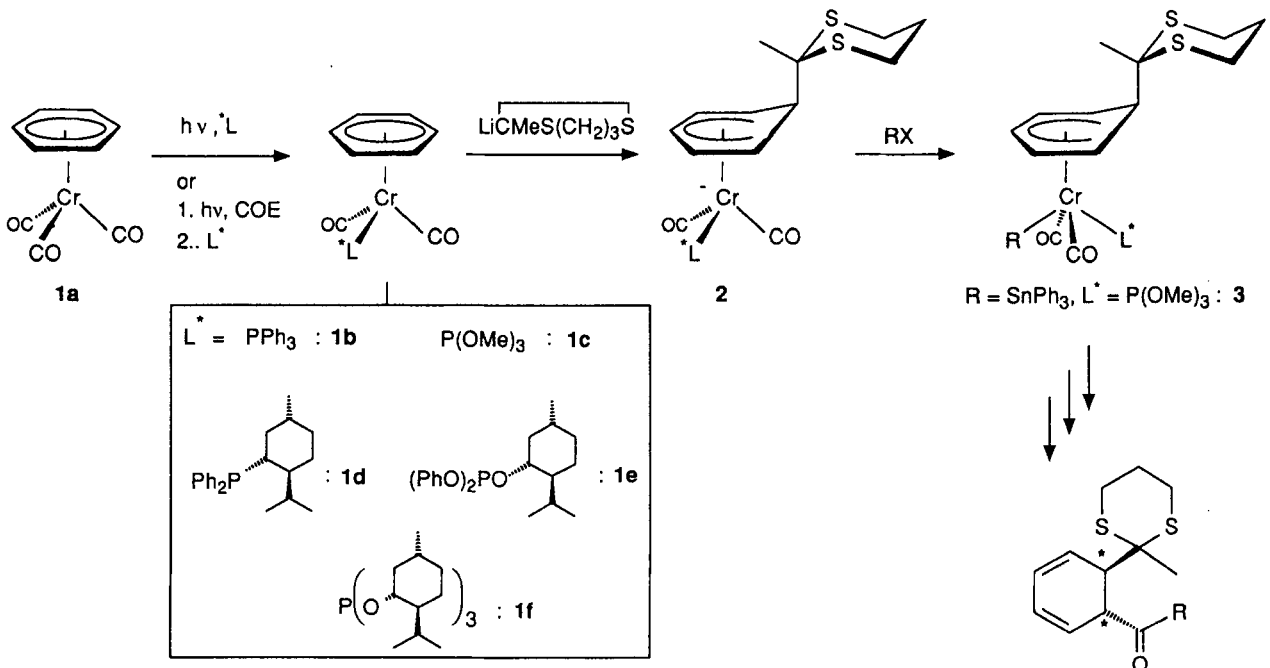

SCHEME II

to gain structural information on the regioselectivity of electrophilic attack, assuming of course that no ligand reorganization takes place after the initial step of this addition mechanism. Interestingly, the X-ray structure of **3a** shows the $[Cr(CO)_3(SnPh_3)]$ fragment in the solid state to be approximately symmetrically oriented with respect to a vertical plane bisecting the cyclohexadienyl through the sp^3 carbon atom and with the $SnPh_3$ ligand trans-oriented to the dithianyl substituent.[68] The result of our modelization is in total agreement with this X-ray structure, as revealed by Fig. 11 which displays the molecular surface of **2a** (L = CO) color-coded according to the reactivity index for electrophilic attack. It is seen indeed in this figure that whereas several sites exhibit a marked preference for such an attack (i.e., the lone pairs of sulfur atoms, the metal and CO ligands), the minimum of E_{int} lies undoubtedly towards the metal, in trans-orientation with respect to the sp^3 carbon of the cyclohexadienyl ligand. Actually, this result is confirmed by further calculations performed using the 3D grid box model instead of the molecular surface: the trans-oriented minimum is roughly 3 kcal/mol lower in energy than the two other ones located on the metal in cis-positions with respect to the dithianyl substituent.

As to complex **3c**, the X-ray structure reported recently reveals that the $Cr-SnPh_3$ bond is trans-located to the phosphite ligand,[70] which again is in agreement with the theoretical result displayed in Fig. 12. This conclusion suggests that our model is able to describe adequately the subtle changes in regioselectivity of the electrophilic attack on **2** induced by replacement of a CO ligand by the more electron rich and bulky $P(OMe)_3$ group. This is probably due to the fact that our E_{es} component, or more generally the MEP property, takes an adequate account of steric effects through the repulsive nuclear contribution of Eq. (2), which allows in turn the E_{int} local reactivity index to reflect the changes induced by ligand substitution.

Phosphine (and to a lesser extent phosphite) derivatives are known to be more electron-rich than carbonyls,[70-72] and consequently their complexes are less susceptible to undergo the first step of the reaction sequence, i.e., nucleophilic attack to **1**. This has been confirmed in our previous study.[70] For the same reason, the resulting anions **2b-2f** are expected to be better nucleophiles

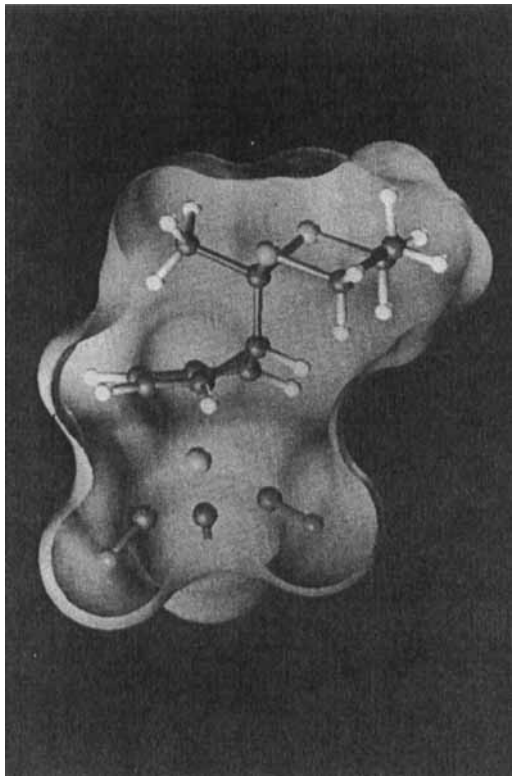

FIGURE 11 Solid model of the molecular surface of the {η^5-[6-(1,3-dithian-2-yl) cyclohexadienyl]$Cr(CO)_3$}$^-$ **2a** complex colored according to the E_{int} reactivity index calculated for electrophilic attack. The most reactive site corresponds to the red zone located towards the metal atom in the trans-position with respect to the CO group eclipsing the sp^3 carbon of the ligand ring. (See Color Plate VII at back of issue.)

than their tricarbonyl counterpart **2a**, i.e., to be more easily attacked by an incoming electrophile. Again, this has been verified experimentally: whereas **2a** requires temperatures near 0° to react with primary alkyl iodides,[68] **2b–2f** can be alkylated at −50°.[70] The values of our E_{int} reactivity index reproduce adequately this trend: whereas the minimum of E_{int} for electrophilic attack of the **2a** anion lies at −239 kcal/mole, it is found at −273 kcal/mol for **2c**, the electrostatic component being responsible as expected for

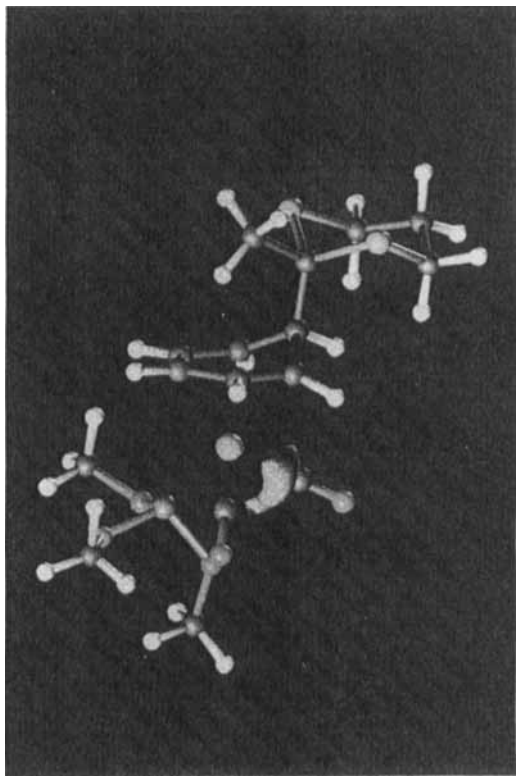

FIGURE 12 Structural model of the $\{\eta^5$-[6-(1,3-dithian-2-yl)cyclohexadienyl]Cr $P(OCH_3)_3(CO)_2\}^-$ **2c** complex represented together with a green-colored solid model of the E_{int} isovalue surface at -250 kcal/mol calculated for electrophilic attack. (See Color Plate VIII at back of issue.)

most of this energy lowering. Of course, these values should be taken cum grano salis as they probably give semi-quantitative information only. However, these results suggest that the E_{int} index can valuably be used to describe the changes in both regioselectivity and reaction rate induced by ligand substitution.

Finally, let us comment briefly on the various energy components of E_{int} calculated for compounds **2a** and **2c** at the minima of this index. Whereas the minimum of E_{int} in the case of **2a** lies at -239 kcal/mol, with $E_{es} = -188$ and $E_{ct} = -51$ kcal/mol, the corresponding values for **2c** are $E_{int} = -273$, $E_{es} = -231$, E_{ct}

−42 kcal/mol. These values suggest that electrostatic interactions are mostly responsible for the nucleophilic character of these complexes, which is not unexpected in view of the negative charge carried by these intermediates. However, charge transfer interactions are not negligible, though taking them into account does not qualitatively change the conclusions drawn from E_{es} alone as far as both regioselectivity and enhanced activity of the phosphine derivative are concerned.

In conclusion, we have shown in this section that our reactivity index is able to describe adequately both the regioselectivity and degree of activation induced by ligand substitution in the case of sequential addition of nucleophiles and electrophiles to complex **1** and related species. Whereas the first part of the reaction sequence, namely the attack by a carbanion nucleophile, takes place on the exo-face of the ligand ring, a metal site is favored in the second addition, in a trans-position to a more bulky, electron rich ligand such as phosphite or, in the case of a $Cr(CO)_3$ moiety, in a trans-position to the sp^3 cyclohexadienyl center. These results, which are in agreement with the X-ray structural properties of the addition products, suggest that our model could be used as a practical tool to rationalize and in some cases predict the characteristics of organometallic reaction mechanisms such as those investigated in the present work.

In any case, the present stage of computational quantum chemistry is such that, for large organometallic systems, it is still difficult to perform state of the art calculations of quantitative value such as those based on MCSCF (+CI)[4,73-75] or even density functional[25,76-78] methodologies, especially when total or partial geometry optimization is required. On the other hand, it is important for chemists to use simple semiempirical procedures leading to qualitative, or at best semiquantitative, information on the structure and reactive properties of such systems. The results reported here suggest that new developments based on well-known quantum chemical methodologies such as EH may still be carried out along these lines. However, in view of the variety and complexity of organometallic reaction mechanisms, there is no doubt that both nonempirical and semiempirical quantum chemical procedures, and probably molecular dynamics techniques as well, will

be required in the near future so as to achieve reliable and comprehensive modelizations in this particular field.

Acknowledgments

The authors are grateful to Professor C. Daul for helpful discussions and to Professor J. Brickmann for providing a copy of the MOLCAD package. This work is part of Projects 20-29856.90 and 20-27940.89 of the Swiss National Science Foundation.

References

1. J. E. Dubois, D. Laurent and J. Weber, Visual Computer **1**, 49 (1985).
2. W. G. J. Hol, Angew. Chem. Int. Ed. Engl. **25**, 767 (1986).
3. H. Frühbeis, R. Klein and H. Wallmeier, Angew. Chem. Int. Ed. Engl. **26**, 403 (1987).
4. E. R. Davidson, in *The Challenge of d and f Electrons. Theory and Computation*, eds. D. R. Salahub and M. C. Zerner, ACS Symp. Ser. **394**, 153 (1989).
5. V. S. Allured, C. M. Kelly and C. R. Landis, J. Am. Chem. Soc. **113**, 1 (1991).
6. U. Burkert and N. L. Allinger, *Molecular Mechanics* (American Chemical Society, Monograph 177, Washington DC, 1982).
7. J. Weber, P. Fluekiger, P. Y. Morgantini, O. Schaad, A. Goursot and C. Daul, J. Comp. Aided Mol. Design **2**, 235 (1988).
8. A. B. Anderson and R. Hoffmann, J. Chem. Phys. **60**, 4271 (1974).
9. G. Calzaferri, L. Forss and I. Kamber, J. Phys. Chem. **93**, 5366 (1989).
10. J. Brickmann, MOLCAD Molecular Modeling Package, Institut für Physikalische Chemie, Technische Hochschule, 6100 Darmstadt, Germany (1989).
11. R. Hoffmann, J. Chem. Phys. **39**, 1397 (1963).
12. E. Scrocco and J. Tomasi, Top. Curr. Chem. **42**, 95 (1973).
13. J. Tomasi, in *Chemical Applications of Atomic and Molecular Electrostatic Potentials*, eds. P. Politzer and D. G. Truhlar (Plenum, New York, 1981), pp. 257–294.
14. H. P. Weber, T. Lybrand, U. Singh and P. A. Kollman, J. Mol. Graphics **4**, 56 (1986).
15. D. A. Brown, N. J. Fitzpatrick and M. A. McGinn, J. Organomet. Chem. **293**, 235 (1985).
16. C. Daul, A. Goursot, P. Y. Morgantini and J. Weber, Int. J. Quantum Chem. **38**, 623 (1990).
17. P. Y. Morgantini, P. Fluekiger, J. Weber and E. P. Kündig, in *Modelling of Molecular Structures and Properties*, ed. J. L. Rivail (Elsevier, Amsterdam, 1990), pp. 313–321.
18. J. Weber, P. Fluekiger, D. Stussi and P. Y. Morgantini, J. Mol. Struct. (Theochem) **221**, 175 (1991).
19. J. Weber, P. Y. Morgantini and O. Einsenstein, J. Mol. Struct. (Theochem) **254**, 343 (1992).

20. Y. Ellinger, R. Subra, G. Berthier and J. Tomasi, J. Phys. Chem. **79**, 2440 (1975).
21. J. Bertran, E. Silla, R. Carbo and M. Martin, Chem. Phys. Lett. **31**, 267 (1975).
22. P. Sjoberg and P. Politzer, J. Phys. Chem. **94**, 3959 (1990).
23. T. M. Chao, J. Baker, W. J. Hehre and S. D. Kahn, Pure & Appl. Chem. **63**, 283 (1991).
24. O. Schaad, M. Roch, H. Chermette and J. Weber, J. Chim. Phys. (Paris) **84**, 829 (1987).
25. P. Jungwirth, D. Stussi and J. Weber, Chem. Phys. Lett. **190**, 29 (1992).
26. M. L. Connolly, Science **221**, 709 (1983).
27. J. Weber, P. Y. Morgantini, P. Fluekiger and A. Goursot, Visual Computer **7**, 158 (1991).
28. E. Surcouf and J. P. Mornon, C. R. Acad. Sci. (Paris) **295**, 923 (1982).
29. J. A. Pople, D. P. Santry and G. A. Segal, J. Chem. Phys. **43**, S129 (1965).
30. A. D. Becke, J. Chem. Phys. **88**, 2547 (1988).
31. P. Sautet, O. Eisenstein and K. M. Nicholas, Organometallics **6**, 1845 (1987).
32. P. Hobza and R. Zahradnik, *Weak Intermolecular Interactions in Chemistry and Biology* (Academia, Prague, 1980), pp. 104–105.
33. *Handbook of Chemistry and Physics* (CRC Press, Boca Raton (Florida) 1987). For H^-, a van der Waals radius of 1.55 Å has been used.
34. E. L. Eliel, N. L. Allinger, S. J. Angyal and G. A. Morrison, *Conformational Analysis* (Wiley, New York, 1965).
35. D. Stussi, Ph.D. thesis in preparation, University of Geneva (1992).
36. E. Clementi and C. Roetti, Atom. Data Nucl. Data Tables **14**, 177 (1974).
37. C. J. Ballhausen and H. B. Gray, *Molecular Orbital Theory* (Benjamin, New York, 1965), p. 125.
38. A. Goursot, F. Fajula, C. Daul and J. Weber, J. Phys. Chem. **92**, 4456 (1988).
39. J. Weber, P. Y. Morgantini, J. Leresche and C. Daul, in *Quantum Chemistry—Basic Aspects, Actual Trends*, ed. R. Carbo (Elsevier, Amsterdam, 1989), pp. 557–576.
40. R. S. Mulliken, J. Chim. Phys. (Paris) **46**, 497 (1949).
41. R. Carbo and M. Martin, Int. J. Quantum Chem. **9**, 193 (1975).
42. O. Mo and M. Yanez, Theoret. Chim. Acta **47**, 263 (1978).
43. J. H. Ammeter, H. B. Bürgi, J. C. Thibeault and R. Hoffmann, J. Am. Chem. Soc. **100**, 3686 (1978).
44. J. C. Culberson and M. C. Zerner, Chem. Phys. Lett. **122**, 436 (1985).
45. S. F. Boys and F. Bernardi, Mol. Phys. **19**, 553 (1970).
46. T. Koga, H. Nakatsuji and T. Yonezawa, Mol. Phys. **39**, 239 (1980).
47. F. Keil and R. Ahlrichs, J. Am. Chem. Soc. **98**, 4787 (1976), and references therein.
48. A. Dedieu and A. Veillard, J. Am. Chem. Soc. **94**, 6730 (1972).
49. M. F. Semmelhack, G. R. Clark, J. L. Garcia, J. J. Harrison, Y. Thebtaranonth, W. Wulff and A. Yamashita, Tetrahedron **37**, 3957 (1981).
50. A. Solladié-Cavallo, Polyhedron **4**, 901 (1985).
51. E. P. Kündig, Pure & Appl. Chem. **57**, 1855 (1985).
52. L. Balas, D. Jhurry, L. Latxague, S. Grelier, Y. Morel, M. Hamdani, N. Ardoin and D. Astruc, Bull. Soc. Chim. Fr. **127**, 401 (1990).
53. M. F. Semmelhack, H. T. Hall, R. Farina, M. Yoshifuji, G. Clark, T. Bargar, K. Hirotsu and J. Clardy, J. Am. Chem. Soc. **101**, 3535 (1979).
54. L. Krumenacker and S. Ratton, Actual. Chim. (Paris) No. 4, 29 (1986).
55. T. F. Block, R. F. Fenske and C. P. Casey, J. Am. Chem. Soc. **98**, 441 (1976).

56. M. F. Semmelhack, G. R. Clark, R. Farina and M. Seaman, J. Am. Chem. Soc. **101**, 217 (1979).
57. D. A. Brown, N. J. Fitzpatrick, M. A. McGinn and T. H. Taylor, Organometallics **5**, 152 (1986).
58. S. D. Kahn, C. F. Pau, L. E. Overman and W. J. Hehre, J. Am. Chem. Soc. **108**, 7381 (1986).
59. D. G. Carroll and S. P. McGlynn, Inorg. Chem. **7**, 1285 (1968).
60. D. A. Brown, J. P. Chester, N. J. Fitzpatrick and I. J. King, Inorg. Chem. **16**, 2497 (1977).
61. T. Albright, P. Hofmann and R. Hoffmann, J. Am. Chem. Soc. **99**, 7546 (1977).
62. T. A. Albright and B. K. Carpenter, Inorg. Chem. **19**, 3092 (1980).
63. J. Y. Saillard, D. Grandjean, F. Choplin and G. Kaufmann, J. Mol. Struct. **23**, 363 (1974).
64. N. J. Fitzpatrick, J. M. Savariault and J. F. Labarre, J. Organomet. Chem. **127**, 325 (1977).
65. M. F. Guest, I. H. Hillier, B. R. Higginson and D. R. Lloyd, Mol. Phys. **29**, 113 (1975).
66. B. Rees and P. Coppens, Acta Cryst. B **29**, 2515 (1973).
67. Y. Wang, K. Angermund, R. Goddard and C. Krüger, J. Am. Chem. Soc. **109**, 587 (1987).
68. E. P. Kündig, A. F. Cunningham, P. Paglia and D. P. Simmons, Helv. Chim. Acta **73**, 386 (1990).
69. E. P. Kündig, M. Inage and G. Bernardinelli, Organometallics **10**, 2921 (1991).
70. G. Bernardinelli, A. Cunningham, C. Dupré, E. P. Kündig, D. Stussi and J. Weber, Chimia **46**, 126 (1992).
71. A. J. Person, *Metallo-organic Chemistry* (Wiley, New York, 1985), pp. 3–5.
72. I. S. Butler and A. A. Ismail, Inorg. Chem. **25**, 3910 (1986).
73. P. O. Widmark, B. O. Roos and P. E. M. Siegbahn, J. Phys. Chem. **89**, 2180 (1985).
74. C. W. Bauschlicher and S. R. Langhoff, Int. Rev. Phys. Chem. **9**, 149 (1990).
75. M. M. Rohmer and M. Bénard, Organometallics **10**, 157 (1991).
76. J. Andzelm, E. Wimmer and D. R. Salahub, in *The Challenge of d and f Electrons. Theory and Computation*, eds. D. R. Salahub and M. C. Zerner, ACS Symp. Ser. **394**, 228 (1989).
77. T. Ziegler, Chem. Rev. **91**, 651 (1991).
78. B. Delley, J. Chem. Phys. **94**, 7245 (1991).